Idaho National Engineering and Environmental Laboratory

INEEL/CON-04-01644
PREPRINT

Critical Heat Flux in Inclined Rectangular Narrow Gaps

Jeong J. Kim – Seoul National University
Yong H. Kim – Seoul National University
Seong J. Kim – Seoul National University
Sang W. Noh – Seoul National University
Kune Y. Suh – Seoul National University
Joy L. Rempe – INEEL
Fan-Bill Cheung – The Pennsylvania State Univ.
Sang B. Kim – Korea Atomic Energy Research Institute

June 13 – 17, 2004

2004 Internation Congress on Advances in Nuclear Power Plants (ICAPP ’04)

Proceedings of ICAPP '04
Pittsburgh, PA, USA, June 13-17, 2004
Paper 4067

Critical Heat Flux in Inclined Rectangular Narrow Gaps

Jeong J. Kim, Yong H. Kim, Seong J. Kim, Sang W. Noh, Kune Y. Suh*
Seoul National University
San 56-1 Sillim-dong, Gwanak-gu, Seoul, 151-742, Korea
**Tel: 82-2-880-8324, Fax: 82-2-889-2688, Email: kysuh@snu.ac.kr*

Joy L. Rempe
Idaho National Engineering & Environmental Laboratory
P.O. Box 1625, Idaho Falls, ID 83415-3840, USA

Fan-Bill Cheung
The Pennsylvania State University
304 Reber Building, University Park, PA 16802, USA

Sang B. Kim
Korea Atomic Energy Research Institute
P.O. Box 105, Yusong, Taejon, Korea, 305-6008

Abstract – *In light of the TMI-2 accident, in which the reactor vessel lower head survived the attack by molten core material, the in-vessel retention strategy was suggested to benefit from cooling the debris through a gap between the lower head and the core material. The GAMMA 1D (Gap Apparatus Mitigating Melt Attack One Dimensional) tests were conducted to investigate the critical heat flux (CHF) in narrow gaps with varying surface orientations. The CHF in an inclined gap, especially in case of the downward-facing narrow gap, is dictated by bubble behavior because the departing bubbles are squeezed. The orientation angle affects the bubble layer and escape of the bubbles from the narrow gap. The test parameters include gap sizes of 1, 2, 5 and 10 mm and the open periphery, and the orientation angles range from the fully downward-facing (180^o) to the vertical (90^o) position. The 15$\times$35 mm copper test section was electrically heated by the thin film resistor on the back. The heater assembly was installed to the tip of the rotating arm in the heated water pool at the atmospheric pressure. The bubble behavior was photographed utilizing a high-speed camera through the Pyrex glass spacer. It was observed that the CHF decreased as the surface inclination angle increased and as the gap size decreased in most of the cases. However, the opposing results were obtained at certain surface orientations and gap sizes. Transition angles, at which the CHF changed in a rapid slope, were also detected, which is consistent with the existing literature. A semi-empirical CHF correlation was developed for the inclined narrow rectangular channels through dimensional analysis. The correlation provides with best-estimate CHF values for realistically assessing the thermal margin to failure of the lower head during a severe accident involving relocation of the core material.*

I. INTRODUCTION

In view of severe accident management for a high power nuclear reactor, it is essential to accurately predict the quantitative magnitude of the critical heat flux (CHF). In the Three-Mile Island Unit 2 (TMI-2) accident, the lower part of the reactor vessel was overheated but then rather rapidly cooled down[1),2)]. This accounted for the possibility of cooling in the narrow gap on the order of millimeters and centimeters that may have been formed between the consolidated core debris and the reactor vessel lower head[3)]. Post-test analyses, completed as part of the TMI-2 Vessel Investigation Project suggested the presence of core material-to-vessel gaps. For this reason, additional data are needed to quantify CHF in narrow gaps and gain insights about the potential for in-vessel retention (IVR).

The CHF test sections need to address key features of the engineering device to simulate the IVR environment. In particular, major issues are centered about geometric parameters affecting the CHF, such as the surface orientation and the gap size. Hence, research on the CHF during pool boiling in confined channels is important as a fundamental study of the CHF phenomenon as well as for its application to industrial problems. In this case, owing to the complexity of flow mode, many investigators have suffered from difficulties in interpreting the heat transfer phenomena in highly confined channels. Additionally, the CHF triggering mechanism still defies full understanding primarily due to the effect of surface orientation. Thus, a series of fundamental studies were conducted to develop engineering correlations taking account of the combined effect of the heated surface orientation and gap size using the apparatus GAMMA 1D (Gap Apparatus Mitigating Melt Attack One Dimensional).

II. EXPERIMENT

In the GAMMA 1D apparatus, heat was supplied by DC power of 6 kW with a DC output voltage of 300 V and a current of 20 A. The quantitative information about the output voltage, ampere and watt generated on the test heater material was exported by the RS-232C to an IBM PC. A quasi-direct heating method was adopted to generate sufficient heat flux in this experiment.

The heater assembly was fabricated utilizing the copper block test heater and the film resistor. A copper block having the wetted surface of 15×35 mm^2 was introduced. Thin film resistors having resistance of 20 ohm were affixed into the copper block heater to measure the CHF. This also facilitated obtaining the required heat flux by applying a current less than 10 A. A schematic diagram of the copper block heater is illustrated in Fig.1, in which chromel-alumel (K-type) thermocouples for measuring the temperature behavior on the wetted surface were inserted into the holes 0.6 mm below the wetted surface. For the test heater used in this study, three K-type thermocouples were inserted into depths of 5, 17.5 and 30 mm, respectively. The test heater was slightly coated with nickel to prevent the test heater from getting oxidized

Regarding the device holding the heater assembly, a stainless steel housing was designed to ensure efficient insulation of the heated section, as illustrated in Fig. 2. The inner surface of the housing was polished smoothly such that the inner of the housing could be evacuated. This allowed an efficient insulation of the heated section. Hence, as part of forming a vacuum, an O-ring frame was grooved in the upper part of the housing, and a link of O-ring was sealed on the housing with vacuum grease. After sticking the copper block heater into the housing, a flexible stainless steel tube was attached to the flange located at the bottom of the housing and a vacuum pump loaded about 10^{-4} torr, which can considerably reduce the heat loss from the bottom of the copper block heater. The conduction heat loss between copper block and housing can be reduced in attaching the high temperature epoxy around the side part of the housing. Pyrex glass was imbedded into the edge of the housing and designed to precisely maintain the gap sizes of 1, 2, 5 and 10 mm, and to visualize the test apparatus having a narrow rectangular channel, as demonstrated in Fig. 2.

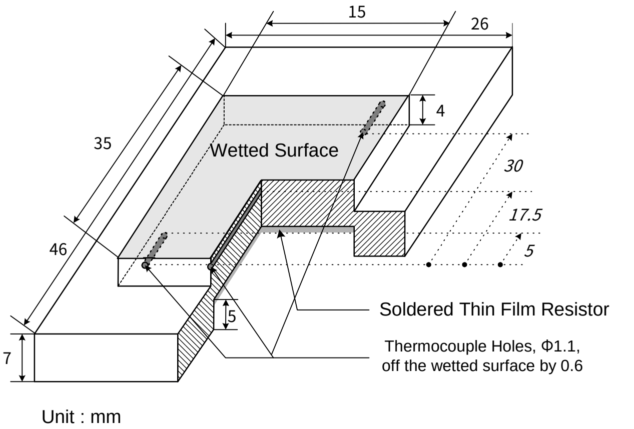

Fig. 1 Test heater block

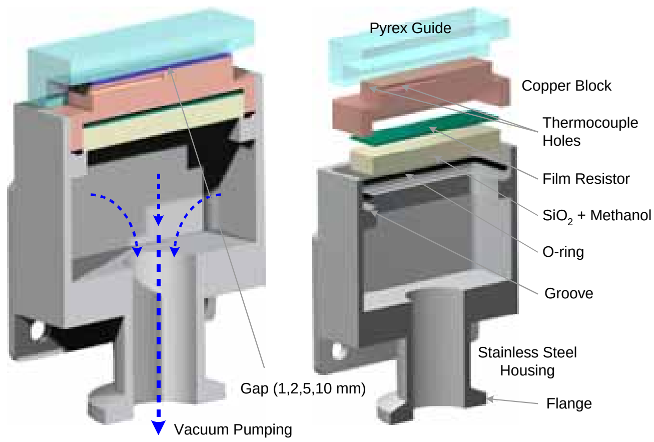

Fig. 2 Test heater with vacuum housing

The CHF tests were performed in the atmosphere water pool surrounded by a vacuum tank, as schematically illustrated in Fig. 3.

In the same way as the housing, the water pool shown in Figs. 4(a) and 4(b) was surrounded by a vacuum for insulation. Additionally, this functions to sustain a steady thermal hydraulic state of water at atmospheric pressure. Eight immersion-type heaters having the electric capacity of 2 kW were homogeneously inserted into the test pool to pre-heat the de-mineralized water in the test pool up to the saturated state. A reflux condenser was equipped in the test pool itself to maintain the pressure in the water pool. After installation was completed for the GAMMA 1D apparatus, the CHF was measured in the narrow channel of the crevice type copper heater block at preset inclination angles at the atmospheric pressure in the water pool. The temperature data were read from the six K-type thermocouples for the bulk fluid utilizing the computer based data acquisition system mainframe of HP VXI-E8406A functioned with the module of HP-1413C. Precise control of the saturated water in the vacuum pool was performed with two temperature controllers. Temperature data readings were 10 times per second, and information was filed to a text file by the HP-VEE 5.0 measurement software.

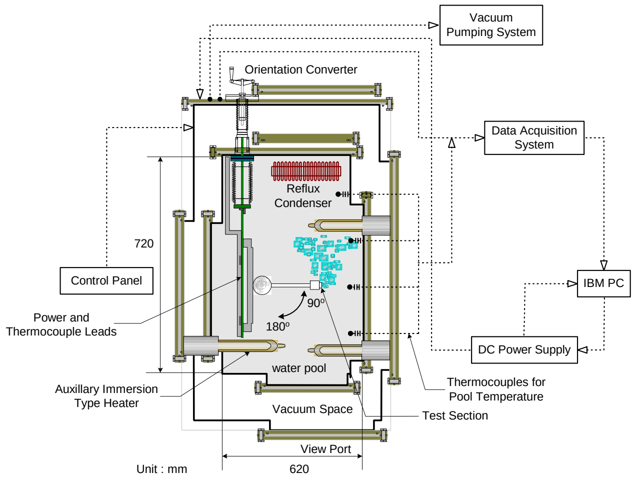

Fig. 3 GAMMA 1D test apparatus

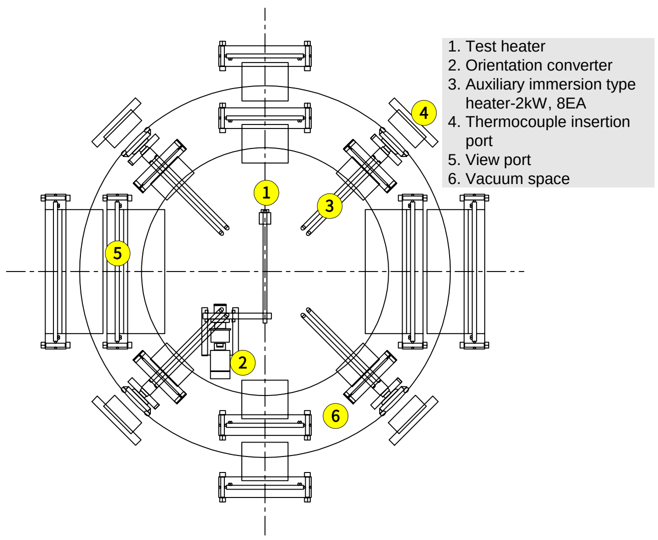

(a) Top view

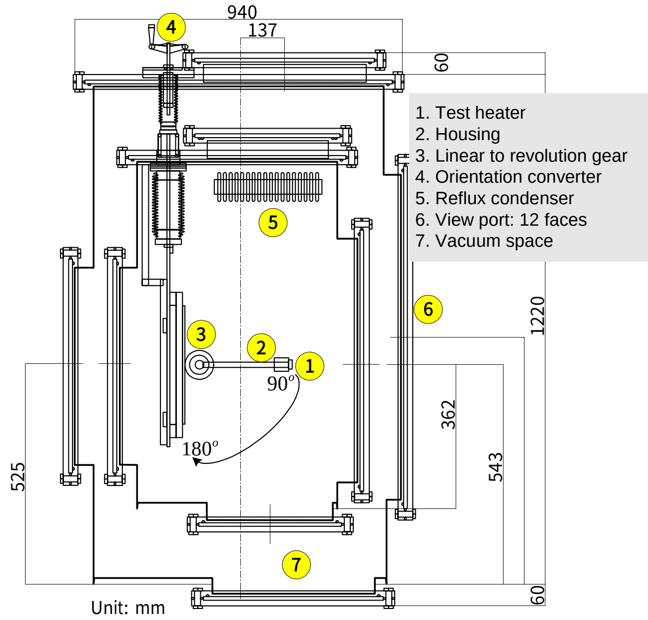

(b) Front view

Fig. 4 GAMMA 1D vacuum water pool

III. RESULTS AND DISCUSSION

III.A. Effect of Gap Size and Surface Orientation Angle

This study is concerned with investigation of the CHF accounting for the gap size and surface orientation effect. Hence, in order to understand the fundamental CHF and related thermal hydraulic phenomena, a one-dimensional test heater assembly was utilized in the experiment to obtain results and to explain the combined effect of gap size and the gravity force in the rectangular channel. Figure 5 shows the CHF data in terms of the gap size and surface inclination angle. The CHF data for pool boiling with an open periphery is depicted in Fig. 6. Visual inspection of the fluid motion in the rectangular channel revealed that the Kelvin-Helmholtz instability was not present in the 1 and 2 mm gaps. However, such instability manifested itself in the 5 and 10 mm gaps at certain angles. For instance, a wavelength of about 21 mm was observed at the vertical position (90^o) in the 10 mm gap.

Generally, the vapor behavior in the narrow gap plays an important role in triggering the CHF. It has generally been claimed that the CHF decreases as the gap size decreases. Contrary to this general knowledge, however, the present study has found opposing results at certain surface inclination angles. At the vertical angle (90^o), for example, in consistency with the general belief, the CHF decreases with the gap size. On the contrary, however, the CHF for the gap size of 10 mm is smaller than that for any other gaps at the fully downward-facing location (180°) as shown in Figs. 5 and 6.

The CHF generally increases as the gap size increases, but the increasing rate decreases with an exception at the fully downward-facing angle as shown in Fig. 5, where the experimental data in this study are compared with other results reported in the literature. In the vertical rectangular geometry of Monde et al.[4)] and Xia et al.[5)], the increasing trend of the CHF with the gap size is compared against the present experimental data. It is found that the CHF changing trend differs with geometry. Though the overall behavior of the CHF in the horizontal co-axial disk is comparable, the CHF is grossly overpredicted. The Monde et al. correlation is found to reasonably represent the current experimental data relatively to the other CHF correlations.

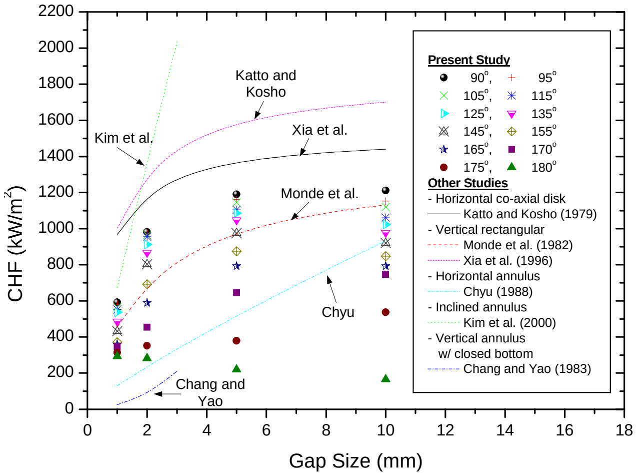

Fig. 5 Effect of gap size on the CHF

The Monde et al. correlation is compared against the CHF data from the gap and pool boiling as shown in Fig. 6(a). Their correlation is found to underestimate the CHF for the 1, 2 and 5 mm gaps. On the other hand, the correlation satisfactorily predicts the CHF data for the 10 mm gap and pool boiling for most of the angles below, say, 150°.

Figures 6(a) and 6(b) show that the CHF for the 1 and 2 mm gaps decreases as the inclination angle increases, and as the gap size decreases except at the fully downward-facing location (180°). At the downward-facing angle, the bubble formed in the gap smaller than its own thickness is affected by the induced flow effect due to the gap structure. To paraphrase, bubbles in the narrow gaps can more easily escape from the restricted channel than those in the larger gaps whose size exceeds the bubble thickness. Though the bubble in the 1, 2 and 5 mm gaps tends to be ejected due to the induced flow, the bubble in the 10 mm gap is stagnated. The induced flow effect increases as the gap size decreases at the fully downward-facing angle. Hence, at the fully downward-facing angle, the CHF decreases as the gap size increases contrary to the trend at other inclination angles. However, the CHF in the pool boiling with an open periphery is greater than the CHF in the gap cooling because the bubble in the pool boiling with an open periphery is free to escape in the azimuthal direction.

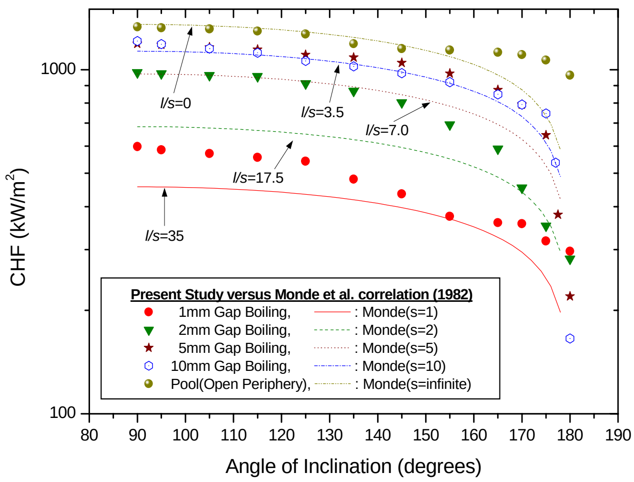

(a) Comparison against the Monde et al. correlation for the gap and pool boiling

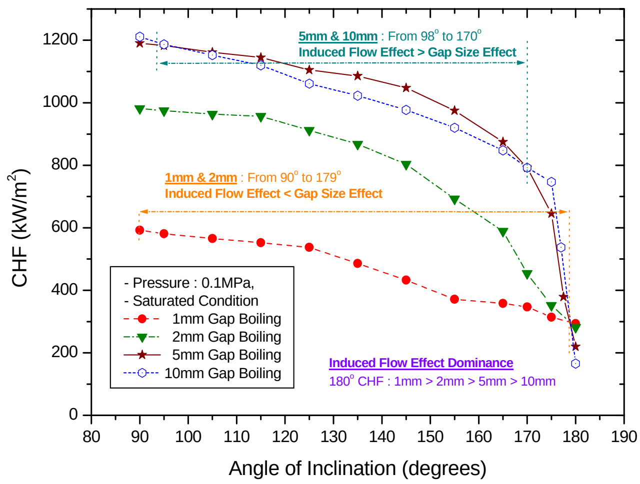

(b) Effect of induced flow and gap size on the CHF in gap boiling

Fig. 6 Effect of surface inclination angle on the CHF

Though the CHF values for the 5 and 10 mm gaps both decrease as the inclination angle increases, the CHF for the 10 mm gap is less than that for the 5 mm gap over a wide range of angles due to absence of the induced flow effect in the 10 mm gap as illustrated in Fig. 6(b). Flow rate depends on the balance between the driving force and pressure drop. The driving force for the 5 mm gap is larger than that for the 10 mm gap on account of high void fraction within the confined channel. Given the flow rate, the pressure drop for the 5 mm gap is greater than that for the 10 mm gap. Then, the mass flux for the 5 mm gap can exceed that for the 10 mm gap due to the smaller flow area over a span of inclination angles. As a result, there appears to be a range of inclination angles over which the CHF increases as the gap decreases. Interestingly enough, this newly theorized thermal hydraulic phenomenon appears to unmistakably take place at the fully downward-facing angle for all the gap sizes examined in this work, and occasionally over some range of angles for the 5 and 10 mm gaps. Therefore, the CHF in the gap boiling is affected by the gap size as well as by the induced flow within the gap.

III.B. Transition Angle

In recent years, some researchers have mentioned the existence of a transition angle at which the CHF changes with a rapid slope. Howard and Mudawar[6)] suggested that based on the vapor behavior observed just prior to the CHF, the surface orientations can be divided into three regions: upward-facing (0^o~60^o), near-vertical (60^o~165^o) and downward-facing (>165^o). Yang et al.[7)] noticed that a transition angle exists in the boiling behavior from vertical-like to downward-facing between 150^o and 174^o. The boundary between the near-vertical and downward-facing regions is generally defined as the transition angle.

In the present study, certain transition angles were also identified for different gap sizes. For the 1 mm gap and pool boiling with open periphery, existence of the transition angle was not discernable as shown in Figs. 7(a) and 7(b). However, in the experiments for the 2, 5 and 10 mm gaps, rather distinct transition angles were observed as captured in Fig. 7(a). For the 2, 5 and 10 mm gaps, the transition angles were found to be 165^o, 170^o and 175^o, respectively. As the CHF is approached, boiling process can be divided into two regions with categorically different slopes in terms of the normalized CHF. In this study, the near-vertical region is defined as the angular range from vertical angle (90^o) to transition and the downward-facing region is defined as the angular span from transition to completely downward-facing location (180^o). Whereas Howard and Mudawar[6)], and Yang et al.[7)] both claimed a transition angle for the pool boiling CHF with open periphery, the current investigation could not necessarily confirm their results. The reason may well be that the aspect ratio of the heater width to length in this study is considerably smaller than that in their experiments. In particular, the heater aspect ratio is 2.3 in this study versus 10.9 and about 10 in Howard and Mudawar[6)], and Yang et al.[7)], respectively. It was also found that the values of $q_{CHF}/q_{CHF,90}$ for differing gap sizes are more broadened as the surface inclination angle increases as shown in Figs. 7(a) and 7(b).

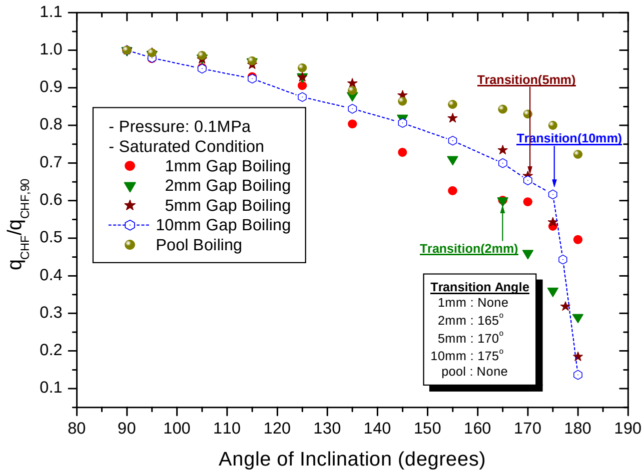

(a) Transition angles for different gaps

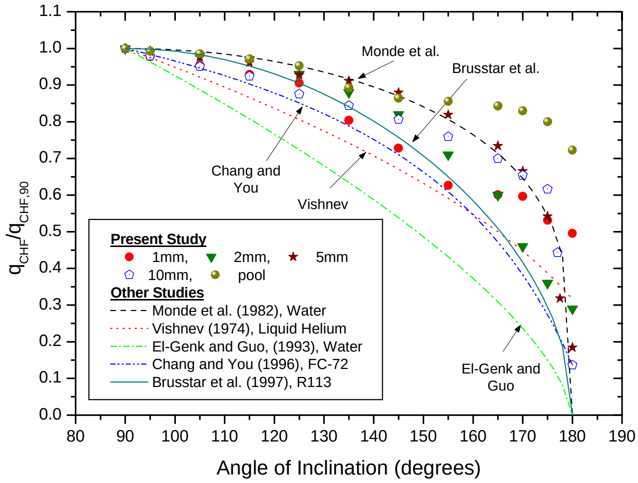

(b) Comparison of present study with other studies

Fig. 7 Effect of surface inclination angle on the normalized CHF values

The normalized CHF data in this work are compared with predictions by the literature correlations developed from tests utilizing such varying fluids as FC-72, water, R113 and liquid helium in Fig. 7(b). The normalized form of the correlations in the cited literature is seen to shift for differing fluids, which appears to support El-Genk and Guo's[8)] assertion that different correlations be used for different fluids in describing the effect of orientation on the CHF. Howard and Mudawar[6)] confirmed different transition angles for different fluids, viz. 150^o for liquid helium, and 160^o to 165^o for water and FC-72. Figure 7(b) suggests that one normalized equation cannot possibly correlate the experimental data at various inclination angles, because the normalized CHF values tend to spread with increasing angles beyond the acceptable error range. That is, the normalized correlation will be affected not only by different fluid properties but also by the surface orientation effect. It is also noted that the Monde et al.[4] and Chang and You[9] correlations provide respectively with the upper and lower bounds for the data taken from the present study.

III.C. Correlation of CHF

It has been shown that surface orientations can be divided into two regions, i.e. near-vertical and downward-facing, each of which is associated with a unique CHF triggering mechanism. For instance, Howard and Mudawar[6] insisted that the vast differences observed between the vapor behavior within the two distinct regions indicate that a single overall pool boiling CHF correlation cannot possibly account for all the observed orientation effect, but instead different models should be developed for the regions. In this study, correlation of the CHF in the near-vertical region is suggested. Monde et al.[4] suggested a generalized correlation of the CHF data in the vertical narrow rectangular channel with the aid of the dimensional analysis developed by Katto[10]. The inclination angle and the heater width were not considered in Monde et al.'s model, though. In this study, their model is modified so as to account implicitly for the effect of the inclination angle and the heater width.

Pursuant to the dimensional analysis by Katto[10], the following correlation can be obtained for the CHF during natural convective boiling in the confined channels in the near-vertical region

$$\frac{q_{CHF}/\rho_g h_{fg}}{\sqrt[4]{\sigma g\sin(\theta)(\rho_f-\rho_g)/\rho_g^2}}=\frac{C_1}{1+C_2(\rho_f/\rho_g)^{C_3}\left(g\sin(\theta)(\rho_f-\rho_g)s^2/\sigma\right)^{C_4}(D_h/s)} \qquad (1)$$

where

$D_h=\dfrac{2wl}{w+l}$ is the equivalent heated surface diameter.

When D_h/s approaches zero, the right side of Eq. (1) is reduced to C_1. This C_1 value corresponds to the constant predicted by Kutateladze[11] as well as by Lienhard and Dhir[12] for the pool boiling CHF in many different geometries. Taking an average for the left side of Eq. (1) for the CHF at all the angles in pool boiling except at 180° in this study, the C_1 value is obtained as 0.17 with the root-mean-square error of 2.4%.

To determine the remaining constants C_2, C_3 and C_4 in Eq. (1), the following form of may be assumed for the CHF data

$$\frac{s}{D_h}\left(\frac{0.17\cdot\sqrt[4]{\sigma g\sin(\theta)(\rho_f-\rho_g)/\rho_g^2}}{q_{CHF}/\rho_g h_{fg}}-1\right)=C_2\left(\frac{\rho_f}{\rho_g}\right)^{C_3}\left(\frac{g\sin(\theta)(\rho_f-\rho_g)s^2}{\sigma}\right)^{C_4} \qquad (2)$$

The CHF data are rearranged as shown in Fig. 8 to evaluate the exponent C_4 in Eq. (2). Figure 8 shows that the left side of Eq. (2) is independent of $g\sin(\theta)(\rho_f-\rho_g)s^2/\sigma$. Then, the value of C_4 is taken as zero. When the least squares method is used for the average value of the CHF for each gap size as well as for the pool boiling, the constants C_2 and C_3 can be obtained. This procedure yields the values of C_2 and C_3 as 6.8×10^{-4} and 0.62, respectively.

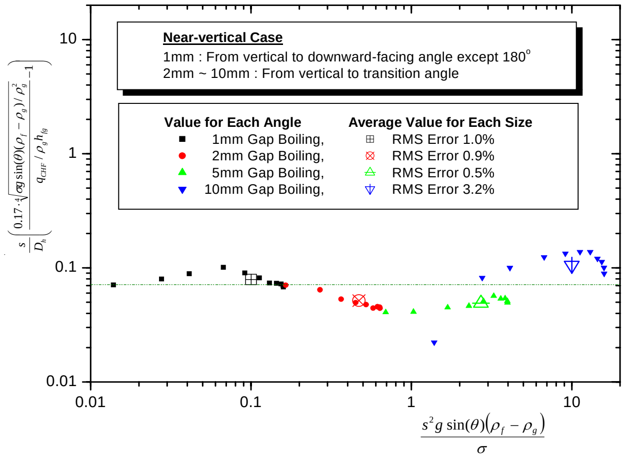

Fig. 8 Effect of the Bond number on the CHF

When the equivalent heated diameter is introduced to account for the width effect, a generalized correlation equation in the near-vertical region based on the CHF data in the present study can be obtained as follows

$$\frac{q_{CHF}/\rho_g h_{fg}}{\sqrt[4]{\sigma g\sin(\theta)(\rho_f-\rho_g)/\rho_g^2}}=\frac{0.17}{1+6.8\times10^{-4}\cdot(\rho_f/\rho_g)^{0.62}(D_h/s)} \qquad (3)$$

Equation (3) turns out to be similar to that due to Monde et al.[4] who had used the aspect ratio of the heated length to the gap size in lieu of the equivalent heated surface diameter to the gap size. Figure 6(a) shows that the Monde et al. correlation underestimates the CHF data for gap boiling in the present study. Figure 9 shows that Eq. (3) predicts the experimental data within an accuracy of ±20%. The CHF data predicted by Eq. (3) are compared against the measured data taken from literature in Fig. 10. It is seen that the developed correlation is in fair agreement with the experimental data of Fujita et al.[13]. Albeit the CHF correlation appears to be in poor agreement with the experimental data of Monde et al.[4] for gap sizes smaller than 1 mm, the developed correlation is in good agreement with the experimental data for gap sizes larger than 1 mm. The smaller the width of flow channel is, the less complex the flow path is. The proposed correlation may not satisfactorily be applied to small gap sizes with small widths, because the CHF in gap sizes smaller than 1 mm with widths smaller than 10 mm may be influenced by the heated length rather than by the equivalent heated surface diameter. However, if the widths exceed 10 mm, the developed correlation may as well be applicable to small gap sizes. Also, Fig.10 compares the developed correlation with the experimental data for the annular tube taken from Kim et al.[14)]. Though the present correlation concurs with the experimental data for the annular tube within a band of ±40%, the constants in Eq. (1) ought to be altered. In the annular tube, the left side of Eq. (2) usually depends on the Bond number $g\sin(\theta)(\rho_f - \rho_g)s^2/\sigma$. The value of C_4 in Eq. (2) is not zero. If dimensional analysis is performed for the experimental data in the annular tube, more accurate prediction may be obtained.

IV. CONCLUSIONS

In this study, the CHF experiments for gap boiling were performed with various gap sizes of 1, 2, 5 and 10 mm, and the heater surface orientations from 90° to 180° in confined narrow space at atmospheric pressure utilizing a rectangular test section. Also, the CHF experiments for pool boiling were carried out with the same heater surface orientations in unconfined space at atmospheric pressure using a rectangular test section. Key conclusions from the study may be summarized as follows.

The CHF generally increases as the gap size increases, but the increasing rate decreases as the gap increases. In particular, the CHF in the 10 mm gap is smaller than the value at any other gap sizes at the fully downward-facing location (180°). At the vertical angle (90°), as is generally believed, the CHF increases as the gap size increases. The CHF in gap boiling is affected by the gap size as well as by the induced flow within the channel.

There is a transition angle for each gap. The transition angle increase as the gap size increases. The transition angles for the 2, 5 and 10 mm gaps were distinctly found to be 165°, 170° and 175°, respectively. However, existence of a transition angle was not discernable for the 1 mm gap and the pool boiling in the unconfined space. The normalized $q_{CHF}/q_{CHF,90}$ values for each gap size at the same angle are more broadened as the surface inclination angle increases.

A semi-empirical CHF correlation was developed for the near-vertical gap boiling using dimensional analysis of the CHF during natural convective boiling in the confined channels because none of the existing correlations could reasonably predict the data obtained in this study. This correlation agrees with the experimental data in this study within ± 20%.

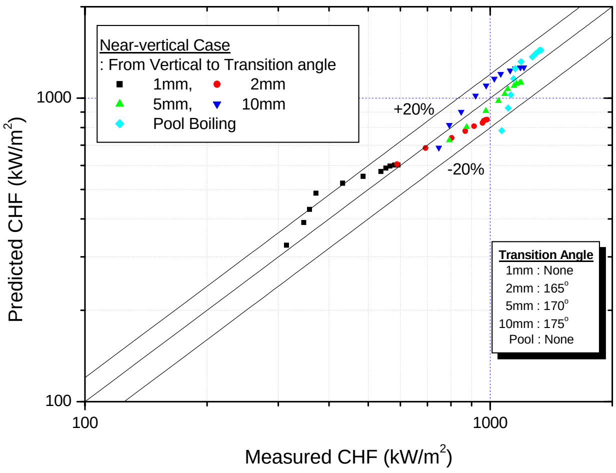

Fig. 9 Comparison between measured and predicted CHF

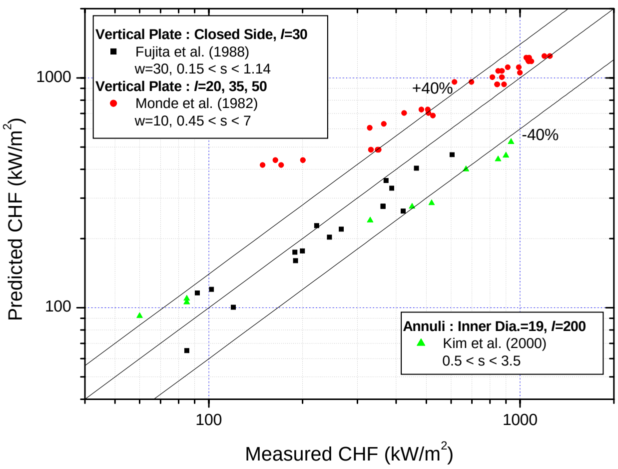

Fig. 10 Comparison of the developed correlation with experimental data from other studies

ACKNOWLEDGMENTS

This work was performed under the auspices of the Ministry of Science and Technology, Korea and the Department of Energy, USA as part of the International Nuclear Energy Research Initiative program awarded to the Seoul National University and the Idaho National Engineering & Environmental Laboratory.

NOMENCLATURE

q_{CHF}	CHF
$q_{CHF,0}$	CHF in ordinary pool boiling on upward-facing position (0°)
$q_{CHF,90}$	CHF in ordinary pool boiling on vertical position (90°)

g gravitational acceleration
h_{fg} latent heat of vaporization
d disk diameter
s channel gap size
l heater length
w channel width size
D_h equivalent heated surface diameter

Greek Letters
θ surface orientation angle
σ surface tension
ρ density

Subscripts
f saturated liquid
g saturated vapor

REFERENCES

1. K. Y. SUH and R. E. Henry, "Debris interactions in reactor vessel lower plena during a severe accident - I. Predictive model," *Nucl. Eng. Des.,* **166**, 147-164 (1996a).

2. K. Y. SUH and R. E. Henry, "Debris interactions in reactor vessel lower plena during a severe accident - II. Integral analysis," *Nucl. Eng. Des.,* **166**, 165-178 (1996b).

3. J. R. WOLF, and J. L. Rempe, "TMI-2 Vessel Investigation Project Integration Report," TMI V(93) EG10, Idaho Falls, ID, USA, October (1993).

4. M. MONDE, H. Kusuda and H. Uehara, "Critical heat flux during natural convective boiling in vertical rectangular channels submerged in saturated liquid," *Trans. ASME, J. Heat Transfer*, **104**, 300-303 (1982).

5. C. XIA, W. Hu and Z. Guo, "Natural convective boiling in vertical rectangular narrow channels," *Experimental Thermal and Fluid Science*, **12**, 313-324 (1996).

6. A. H. HOWARD and I. Mudawar, "Orientation Effects on Pool Boiling Critical Heat Flux (CHF) and Modeling of CHF for Near-Vertical Surfaces," *Int. J. Heat Mass Transer,* **42**, 1665-1688 (1999).

7. S. H. YANG, W. P. Baek and S. H. Chang, "Pool-boiling critical heat flux of water on small plates: Effects of surface orientation and size," *Int. Comm. Heat Mass Transfer*, **24**, 1093-1102 (1997).

8. M. S. EL-GENK and Z. Guo, "Transient boiling from inclined and downward-facing surfaces in a saturated pool," *Int. J. Refrigeration,* **6**, 424-432 (1993).

9. J. Y. CHANG and S. M. You, "Heater orientation effects on pool boiling of micro-porous-enhanced surfaces in saturated FC-72," *Trans. ASME, J. Heat Transfer,* **118**, 937-943 (1996).

10. Y. KATTO, "Generalized correlation for critical heat flux of natural convective boiling in confined channels," *Trans. JSME (in Japanese),* **44**, 3908-3911 (1978).

11. S. S. KUTATELADZE, "Heat transfer in condensation and boiling," *AEC-TR-3770* (1952).

12. J. H. LIENHARD and V. K. Dhir, "Hydrodynamic prediction of peak pool-boiling heat fluxes from finite bodies," *ASME J. Heat Transfer,* **95**, 152-158 (1973).

13. Y. FUJITA, H. Ohta, S.Uchida and K. Nishikawa, "Nucleate boiling heat transfer and critical heat flux in narrow space between rectangular surfaces," *Int. J. Heat Mass Transfer,* **31**, 229-239 (1988).

14. S. H. KIM, W. P., Baek, S. H. Chang, "Measurements of critical heat flux for narrow annuli submerged in saturated water," *Nucl. Eng. Des.,* **199**, 41-48 (2000).